

# Discovery of the spectroscopic binary nature of three bright southern Cepheids

L. Szabados,<sup>1</sup>\* R. I. Anderson,<sup>2</sup> A. Derekas,<sup>1,3</sup> L. L. Kiss,<sup>1,3,4</sup> T. Szalai,<sup>5</sup> P. Székely<sup>6</sup> and J. L. Christiansen<sup>7</sup>

<sup>1</sup>Konkoly Observatory, Research Centre for Astronomy and Earth Sciences, Hungarian Academy of Sciences, Konkoly Thege Miklós út 15-17, H-1121 Budapest, Hungary

<sup>2</sup>Observatoire de Genève, Université de Genève, 51 Ch. des Maillettes, CH-1290 Versoix, Switzerland

<sup>3</sup>Sydney Institute for Astronomy, School of Physics, University of Sydney, NSW 2006, Australia

<sup>4</sup>ELTE Gothard–Lendület Research Group, Szent Imre herceg út 112, H-9700 Szombathely, Hungary

<sup>5</sup>Department of Optics and Quantum Electronics, University of Szeged, Dóm tér 9, H-6720 Szeged, Hungary

<sup>6</sup>Department of Experimental Physics, University of Szeged, H-6720 Szeged, Hungary

<sup>7</sup>SETI Institute/NASA Ames Research Center, M/S 244-30, Moffett Field, CA 94035, USA

Accepted 2013 June 13. Received 2013 June 13; in original form 2013 May 14

## ABSTRACT

We present an analysis of spectroscopic radial velocity and photometric data of three bright Galactic Cepheids: LR Trianguli Australis (LR TrA), RZ Velorum (RZ Vel) and BG Velorum (BG Vel). Based on new radial velocity data, these Cepheids have been found to be members of spectroscopic binary systems. The ratio of the peak-to-peak radial velocity amplitude to photometric amplitude indicates the presence of a companion for LR TrA and BG Vel. *IUE* spectra indicate that the companions of RZ Vel and BG Vel cannot be hot stars. The analysis of all available photometric data revealed that the pulsation period of RZ Vel and BG Vel varies monotonically, due to stellar evolution. Moreover, the longest period Cepheid in this sample, RZ Vel, shows period fluctuations superimposed on the monotonic period increase. The light-time effect interpretation of the observed pattern needs long-term photometric monitoring of this Cepheid. The pulsation period of LR TrA has remained constant since the discovery of its brightness variation. Using statistical data, it is also shown that a large number of spectroscopic binaries still remain to be discovered among bright classical Cepheids.

**Key words:** binaries: spectroscopic – stars: variables: Cepheids.

## 1 INTRODUCTION

Classical Cepheid variable stars are primary distance indicators and rank among standard candles for establishing the cosmic distance scale, owing to the famous period–luminosity ( $P$ – $L$ ) relationship. Companions to Cepheids, however, complicate the situation. The contribution of the secondary star to the observed brightness has to be taken into account when involving any particular Cepheid in the calibration of the  $P$ – $L$  relationship.

Binaries among Cepheids are not rare at all: their frequency exceeds 50 per cent for the brightest Cepheids, while among the fainter Cepheids an observational selection effect encumbers revealing binarity (Szabados 2003a).

Owing to some observational projects, aimed at obtaining new radial velocities (RVs) of numerous Cepheids, carried out during the last decades, a part of the selection effect has been removed.

This progress is visualized in Fig. 1 where the current situation is compared with that 20 years ago. The data have been taken from the online data base of binaries among Galactic Cepheids (<http://www.konkoly.hu/CEP/orbit.html>). To get rid of the fluctuation at the left-hand part of the diagram, brightest Cepheids ( $\langle V \rangle < 5$  mag) were merged in a single bin because such stars are extremely rare among Cepheids – see the histogram in Fig. 2.

In the case of pulsating variables, like Cepheids, spectroscopic binarity manifests itself in a periodic variation of the  $\gamma$ -velocity (i.e. the RV of the mass centre of the Cepheid). In practice, the orbital RV variation of the Cepheid component is superimposed on the RV variations of pulsational origin. To separate orbital and pulsational effects, knowledge of the accurate pulsation period is essential, especially when comparing RV data obtained at widely differing epochs. Therefore, the pulsation period and its variations have been determined with the method of the O–C diagram (Sterken 2005) for each target Cepheid. Use of the accurate pulsation period obtained from the photometric data is a guarantee for the correct phase matching of the (usually less precise) RV data.

\* E-mail: szabados@konkoly.hu

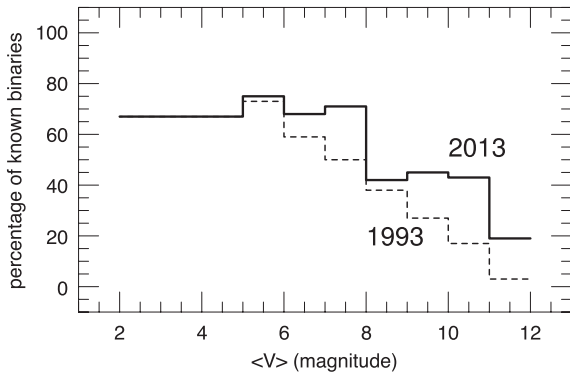


**Figure 1.** Percentage of known binaries among Galactic classical Cepheids as a function of the mean apparent visual brightness in 1993 and 2013. The decreasing influence of the observational selection effect is noticeable.

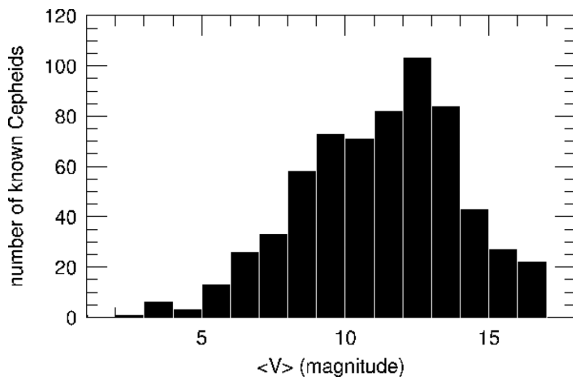


**Figure 2.** Histogram showing the number distribution of known Galactic classical Cepheids as a function of their mean apparent visual brightness.

In this paper, we point out spectroscopic binarity of three bright Galactic Cepheids by analysing RV data. The structure of this paper is as follows. The new observations and the equipment utilized are described in Section 2. Section 3 is devoted to the results on the three new spectroscopic binary (SB) Cepheids: LR Trianguli Australis (LR TrA), RZ Velorum (RZ Vel) and BG Velorum (BG Vel). Basic information on these Cepheids is given in Table 1. Finally, Section 4 contains our conclusions.

## 2 NEW OBSERVATIONS

### 2.1 Spectra from the Siding Spring Observatory

We performed an RV survey of Cepheids with the 2.3-m ANU telescope located at the Siding Spring Observatory (SSO), Australia. The main aim of the project was to detect Cepheids in binary systems by measuring changes in the mean values of their RV curve which can be interpreted as the orbital motion of the Cepheid around the centre-of-mass in a binary system (change of  $\gamma$ -velocity). The target list was compiled to include Cepheids with a single-epoch RV phase

**Table 1.** Basic data of the programme stars and the number of spectra.

| Cepheid | $\langle V \rangle$<br>(mag) | $P$<br>(d) | Mode of pulsation | Number of spectra |         |
|---------|------------------------------|------------|-------------------|-------------------|---------|
|         |                              |            |                   | SSO               | CORALIE |
| LR TrA  | 7.80                         | 2.428 289  | First overtone    | 10                | 32      |
| RZ Vel  | 7.13                         | 20.398 532 | Fundamental       | 30                | 67      |
| BG Vel  | 7.69                         | 6.923 843  | Fundamental       | 27                | 33      |

curve or without any published RV data. Several Cepheids suspected to be members of SB systems were also put on the target list. In 64 nights between 2004 October and 2006 March we monitored 40 Cepheids with pulsation periods between 2 and 30 d. Additional spectra of some targets were obtained in 2007 August.

Medium-resolution spectra were taken with the Double Beam Spectrograph using the  $1200 \text{ mm}^{-1}$  gratings in both arms of the spectrograph. The projected slit width was 2 arcsec on the sky, which was about the median seeing during our observations. The spectra covered the wavelength ranges  $4200\text{--}5200 \text{ \AA}$  in the blue arm and  $5700\text{--}6700 \text{ \AA}$  in the red arm. The dispersion was  $0.55 \text{ \AA pixel}^{-1}$ , leading to a nominal resolution of about  $1 \text{ \AA}$ .

All spectra were reduced with standard tasks in IRAF.<sup>1</sup> The reduction consisted of bias and flat-field corrections, aperture extraction, wavelength calibration and continuum normalization. We checked the consistency of wavelength calibrations via the constant positions of strong telluric features, which proved the stability of the system. RVs were determined only for the red arm data with the task `fxcor`, applying the cross-correlation method using a well-matching theoretical template spectrum from the extensive spectral library of Munari et al. (2005). Then, we made barycentric corrections to every single RV value. This method resulted in a  $1\text{--}2 \text{ km s}^{-1}$  uncertainty in the individual RVs, while further tests have shown that our absolute velocity frame was stable to within  $\pm 2\text{--}3 \text{ km s}^{-1}$ . This level of precision is sufficient to detect a number of Cepheid companions, as they can often cause  $\gamma$ -velocity changes well above  $10 \text{ km s}^{-1}$ .

Discovery of six SBs among the 40 target Cepheids was already reported by Szabados et al. (2013). The binarity of the three Cepheids announced here could be revealed by involving independently obtained additional data (see Section 2.2). The individual RV data of the rest of the Cepheid targets will be published together with the results of the analysis of the spectra.

### 2.2 CORALIE observations from La Silla

All three Cepheids were among the targets during multiple observing campaigns between 2011 April and 2012 May using the fibre-fed high-resolution ( $R \sim 60\,000$ ) echelle spectrograph CORALIE mounted on the Swiss 1.2-m Euler telescope at the ESO La Silla Observatory, Chile. The instrument's design is described in Queloz et al. (2001); recent instrumental updates can be found in Ségransan et al. (2010).

When it turned out that these three Cepheids have variable  $\gamma$ -velocities, several new spectra were obtained in 2012 December–2013 January and 2013 April.

The spectra are reduced by the efficient online reduction pipeline that performs bias correction, cosmics removal and flat-fielding using tungsten lamps. ThAr lamps are used for the wavelength calibration. The reduction pipeline directly determines the RV via cross-correlation (Baranne et al. 1996) using a mask that resembles a G2 spectral type. The RV stability of the instrument is excellent and for non-pulsating stars the RV precision is limited by photon noise (see e.g. Pepe et al. 2002). However, the precision achieved for Cepheids is lower due to line asymmetries. We estimate a typical precision of  $\sim 0.1 \text{ km s}^{-1}$  (including systematics due to pulsation) per data point for our data.

<sup>1</sup> IRAF is distributed by the National Optical Astronomy Observatories, which are operated by the Association of Universities for Research in Astronomy, Inc., under cooperative agreement with the National Science Foundation.

### 3 RESULTS FOR INDIVIDUAL CEPHEIDS

#### 3.1 LR Trianguli Australis

*Accurate value of the pulsation period.* The brightness variability of LR TrA (HD 137626,  $\langle V \rangle = 7.80$  mag) was revealed by Strohmeier, Fischer & Ott (1966) based on the Bamberg photographic patrol plates. The Cepheid nature of variability and the first values of the pulsation period were determined by Eggen (1983). This Cepheid pulsates in the first-overtone mode; therefore, it has a small pulsational amplitude and nearly-sinusoidal light and velocity curves.

In the case of Cepheids pulsating with a low amplitude, the O–C diagram constructed for the median brightness (the mid-point between the faintest and the brightest states) is more reliable than that based on the moments of photometric maxima (Derekas et al. 2012). Therefore, we determined the accurate value of the pulsation period by constructing an O–C diagram for the moments of median brightness on the ascending branch of the light curve since this is the phase when the brightness variations are steepest during the whole pulsational cycle.

All published photometric observations of LR TrA covering three decades were re-analysed in a homogeneous manner to determine seasonal moments of the chosen light-curve feature. The relevant data listed in Table 2 are as follows:

Column 1: heliocentric moment of the selected light-curve feature (median brightness on the ascending branch for LR TrA, maximum brightness for both RZ Vel and BG Vel, see Tables 6 and 10, respectively);

Column 2: epoch number,  $E$ , as calculated from equation (1):

$$C = 245\,3104.9265 + 2.428\,289 \times E \pm 0.0037 \pm 0.000\,003 \quad (1)$$

(this ephemeris has been obtained by the weighted least-squares parabolic fit to the O–C differences);

**Table 2.** O–C values of LR TrA (see the description in Section 3.1).

| JD <sub>⊙</sub><br>240 0000 + | $E$   | O–C     | $W$ | Data source                         |
|-------------------------------|-------|---------|-----|-------------------------------------|
| 450 18.7822                   | –3330 | 0.0581  | 3   | Eggen (1983)                        |
| 476 33.9607                   | –2253 | –0.0307 | 3   | Antonello, Poretti & Reduzzi (1990) |
| 479 39.9568                   | –2127 | 0.0010  | 2   | <i>Hipparcos</i> (ESA 1997)         |
| 481 39.0426                   | –2045 | –0.0329 | 3   | <i>Hipparcos</i> (ESA 1997)         |
| 484 40.1554                   | –1921 | –0.0279 | 3   | <i>Hipparcos</i> (ESA 1997)         |
| 487 50.9547                   | –1793 | –0.0496 | 3   | <i>Hipparcos</i> (ESA 1997)         |
| 498 14.6064                   | –1355 | 0.0115  | 3   | Berdnikov (2008)                    |
| 503 70.7115                   | –1126 | 0.0384  | 3   | Berdnikov (2008)                    |
| 505 74.6393                   | –1042 | –0.0101 | 3   | Berdnikov (2008)                    |
| 509 09.7531                   | –904  | –0.0001 | 3   | Berdnikov (2008)                    |
| 512 64.2883                   | –758  | 0.0049  | 3   | Berdnikov (2008)                    |
| 516 50.4058                   | –599  | 0.0244  | 3   | Berdnikov (2008)                    |
| 519 58.8010                   | –472  | 0.0269  | 2   | Berdnikov (2008)                    |
| 520 41.3435                   | –438  | 0.0076  | 2   | ASAS (Pojmanski 2002)               |
| 523 66.7222                   | –304  | –0.0044 | 3   | Berdnikov (2008)                    |
| 525 00.2709                   | –249  | –0.0116 | 3   | ASAS (Pojmanski 2002)               |
| 527 69.8038                   | –138  | –0.0188 | 3   | ASAS (Pojmanski 2002)               |
| 531 02.5159                   | –1    | 0.0177  | 3   | Berdnikov (2008)                    |
| 531 04.9151                   | 0     | –0.0114 | 3   | ASAS (Pojmanski 2002)               |
| 535 20.1818                   | 171   | 0.0179  | 3   | ASAS (Pojmanski 2002)               |
| 538 40.7137                   | 303   | 0.0156  | 3   | ASAS (Pojmanski 2002)               |
| 542 51.0850                   | 472   | 0.0061  | 3   | ASAS (Pojmanski 2002)               |
| 546 15.3163                   | 622   | –0.0060 | 3   | ASAS (Pojmanski 2002)               |
| 549 60.1214                   | 764   | –0.0179 | 3   | ASAS (Pojmanski 2002)               |

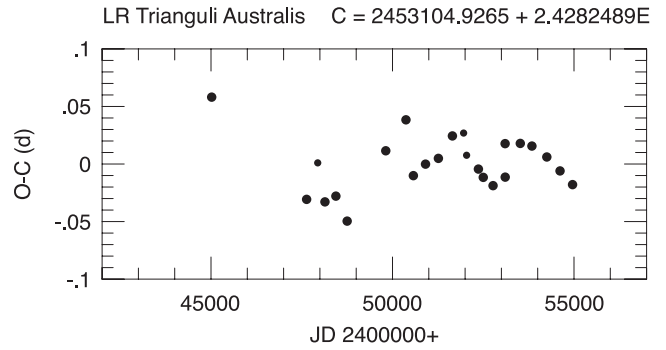


**Figure 3.** O–C diagram of LR TrA. The plot can be approximated by a constant period.

Column 3: the corresponding O–C value;

Column 4: weight assigned to the O–C value (1, 2 or 3 depending on the quality of the light curve leading to the given difference);

Column 5: reference to the origin of data.

The O–C diagram of LR TrA based on the O–C values listed in Table 2 is plotted in Fig. 3. The plot can be approximated by a constant period by the ephemeris (1) for the moments of median brightness on the ascending branch. The scatter of the points in Fig. 3 reflects the observational error and uncertainties in the analysis of the data.

*Binarity of LR TrA.* There are no earlier RV data on this bright Cepheid. Our new data listed in Tables 3 and 4 have been folded on the accurate pulsation period given in the ephemeris (see equation 1). The merged RV phase curve is plotted in Fig. 4. Both individual data series could be split into seasonal subsets.

Variability in the  $\gamma$ -velocity is obvious. The  $\gamma$ -velocities (together with their uncertainties) are listed in Table 5. The  $\gamma$ -velocity in 2007 is more uncertain than in other years because this value is based on a single spectrum. Systematic errors can be excluded. Dozens of Cepheids in our sample with non-varying  $\gamma$ -velocities

**Table 3.** RV values of LR TrA from the SSO spectra. (This is only a portion of the full version available online as Supporting Information.)

| JD <sub>⊙</sub><br>2 400 000 + | $v_{\text{rad}}$<br>(km s <sup>–1</sup> ) |
|--------------------------------|---|
| 535 99.9325                    | –21.2                                     |
| 536 00.9086                    | –32.0                                     |
| 536 03.9327                    | –27.6                                     |
| 536 05.9290                    | –31.0                                     |
| 538 05.1657                    | –29.3                                     |
| ...                            | ...                                       |

**Table 4.** CORALIE velocities of LR TrA. (This is only a portion of the full version available online as Supporting Information.)

| JD <sub>⊙</sub><br>240 0000 + | $v_{\text{rad}}$<br>(km s <sup>–1</sup> ) | $\sigma$<br>(km s <sup>–1</sup> ) |
|-------------------------------|---|-----------------------------------|
| 559 38.8701                   | –27.97                                    | 0.05                              |
| 559 38.8718                   | –28.10                                    | 0.05                              |
| 559 39.8651                   | –29.85                                    | 0.02                              |
| 559 40.8686                   | –22.40                                    | 0.03                              |
| 559 41.8579                   | –33.14                                    | 0.04                              |
| ...                           | ...                                       | ...                               |

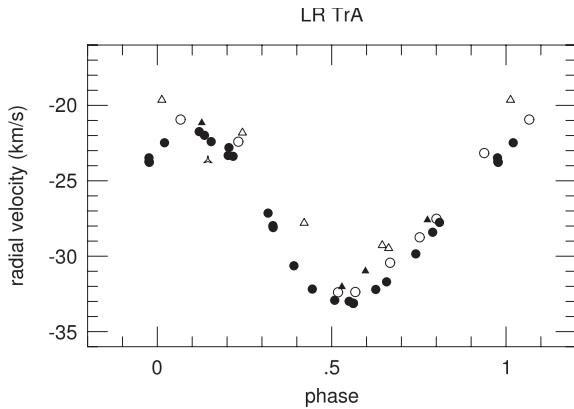


**Figure 4.** Merged RV phase curve of LR TrA. The different symbols mean data from different years: 2005: filled triangles; 2006: empty triangles; 2007: triangular star; 2012: filled circles; 2013: empty circles. The zero phase was arbitrarily chosen at JD 240 0000.0 (in all phase curves in this paper).

**Table 5.**  $\gamma$ -velocities of LR TrA.

| Mid-JD<br>240 0000+ | $v_\gamma$<br>(km s <sup>-1</sup> ) | $\sigma$<br>(km s <sup>-1</sup> ) | Data source   |
|---------------------|-------------------------------------|-----------------------------------|---------------|
| 536 03              | -25.5                               | 0.5                               | Present paper |
| 538 08              | -24.8                               | 0.5                               | Present paper |
| 543 31              | -29.0                               | 1.0                               | Present paper |
| 559 81              | -27.5                               | 0.1                               | Present paper |
| 563 44              | -26.4                               | 0.1                               | Present paper |

indicate the stability of the equipment and reliability of the data reduction. Fig. 5 is a better visualization of the temporal variation in the  $\gamma$ -velocity. The seasonal drift in the  $\gamma$ -velocity is compatible with both short and long orbital periods.

The photometric contribution of the companion star decreases the observable amplitude of the brightness variability as deduced from the enhanced value of the ratio of the RV to photometric amplitudes (Klagyivik & Szabados 2009). This is an additional (although slight) indication of the binarity of LR TrA.

### 3.2 RZ VELORUM

*Accurate value of the pulsation period.* The brightness variability of RZ Vel (HD 73502,  $\langle V \rangle = 7.13$  mag) was revealed by Cannon (Pickering 1909). The Cepheid nature of variability and the pulsation period were established by Hertzsprung (1936) based on the

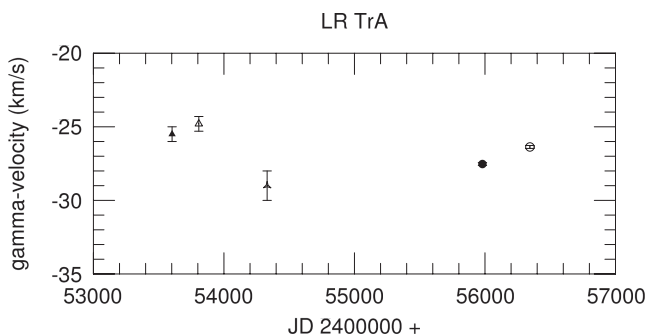


**Figure 5.** Temporal variation in the  $\gamma$ -velocity of LR TrA. The symbols for the different data sets are the same as in Fig. 4.

Harvard and Johannesburg photographic plate collection which was further investigated by Oosterhoff (1936).

This is the longest period Cepheid announced in this paper and it has been frequently observed from the 1950s, first photoelectrically, then in the last decades by CCD photometry. The photometric coverage of RZ Vel was almost continuous in the last 20 years, thanks to observational campaigns by Berdnikov (2008) and his co-workers, as well as the ASAS photometry (Pojmanski 2002).

Long-period Cepheids are usually fundamental pulsators and they oscillate with a large amplitude, resulting in a light curve with sharp maximum.

The O–C diagram of RZ Vel was constructed for the moments of maximum brightness based on the photoelectric and CCD photometric data (see Table 6). The weighted least-squares parabolic fit to the O–C values resulted in the ephemeris:

$$C = 244\,2453.6630 + 20.398\,532 \times E + 1.397 \times 10^{-6} E^2 \pm 0.0263 \pm 0.000\,080 \pm 0.191 \times 10^{-6} \quad (2)$$

The O–C diagram of RZ Vel plotted in Fig. 6 indicates a continuously increasing pulsation period with a period jitter superimposed. This secular period increase has been caused by stellar evolution: while the Cepheid crosses the instability region towards lower temperatures in the Hertzsprung–Russell diagram, its pulsation period

**Table 6.** O–C values of RZ Vel (description of the columns is given in Section 3.1).

| JD <sub>⊙</sub><br>240 0000 + | $E$  | O–C     | $W$ | Data source                          |
|-------------------------------|------|---------|-----|--------------------------------------|
| 337 84.5646                   | −425 | 0.2777  | 1   | Eggen, Gascoigne & Burr (1957)       |
| 348 04.5174                   | −375 | 0.3039  | 1   | Walraven, Muller & Oosterhoff (1958) |
| 348 45.2119                   | −373 | 0.2013  | 3   | Eggen et al. (1957)                  |
| 351 92.0024                   | −356 | 0.2168  | 1   | Irwin (1961)                         |
| 407 60.8647                   | −83  | 0.2799  | 3   | Pel (1976)                           |
| 417 19.0924                   | −36  | −0.2234 | 3   | Madore (1975)                        |
| 418 62.1249                   | −29  | 0.0193  | 3   | Dean et al. (1977)                   |
| 424 53.6330                   | 0    | −0.0030 | 3   | Dean et al. (1977)                   |
| 443 71.0472                   | 94   | −0.0778 | 3   | Coulson & Caldwell (1985)            |
| 443 91.3842                   | 95   | −0.1393 | 2   | Eggen (1982)                         |
| 450 03.2906                   | 125  | −0.1889 | 3   | Coulson & Caldwell (1985)            |
| 482 26.4369                   | 283  | −0.0107 | 3   | <i>Hipparcos</i> (ESA 1997)          |
| 487 97.5877                   | 311  | −0.0188 | 3   | <i>Hipparcos</i> (ESA 1997)          |
| 491 85.1653                   | 330  | −0.0133 | 1   | Walker & Williams (unpublished)      |
| 498 17.8011                   | 361  | 0.2680  | 3   | Berdnikov (2008)                     |
| 501 44.1979                   | 377  | 0.2883  | 2   | Bersier (2002)                       |
| 503 89.0443                   | 389  | 0.3524  | 3   | Berdnikov (2008)                     |
| 505 11.3662                   | 395  | 0.2831  | 3   | Bersier (2002)                       |
| 505 72.4468                   | 398  | 0.1681  | 3   | Berdnikov (2008)                     |
| 508 99.0581                   | 414  | 0.4029  | 3   | Berdnikov (2008)                     |
| 512 66.1488                   | 432  | 0.3200  | 3   | Berdnikov (2008)                     |
| 516 53.7650                   | 451  | 0.3641  | 3   | Berdnikov (2008)                     |
| 519 39.2846                   | 465  | 0.3042  | 2   | ASAS (Pojmanski 2002)                |
| 519 59.7692                   | 466  | 0.3903  | 3   | Berdnikov (2008)                     |
| 523 47.4262                   | 485  | 0.4752  | 3   | Berdnikov (2008)                     |
| 526 53.3896                   | 500  | 0.4606  | 3   | ASAS (Pojmanski 2002)                |
| 526 53.4100                   | 500  | 0.4810  | 3   | Berdnikov (2008)                     |
| 530 00.1794                   | 517  | 0.4754  | 3   | ASAS (Pojmanski 2002)                |
| 530 00.2610                   | 517  | 0.5570  | 3   | Berdnikov (2008)                     |
| 534 28.4384                   | 538  | 0.3652  | 3   | ASAS (Pojmanski 2002)                |
| 537 54.8864                   | 554  | 0.4367  | 3   | ASAS (Pojmanski 2002)                |
| 541 83.1657                   | 575  | 0.3468  | 3   | ASAS (Pojmanski 2002)                |
| 545 09.5729                   | 591  | 0.3775  | 3   | ASAS (Pojmanski 2002)                |
| 548 15.4343                   | 606  | 0.2609  | 3   | ASAS (Pojmanski 2002)                |
| 551 21.3569                   | 621  | 0.2055  | 2   | ASAS (Pojmanski 2002)                |

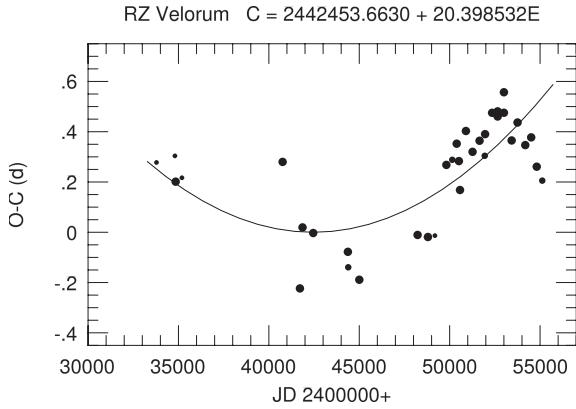


**Figure 6.** O–C diagram of RZ Vel. The plot can be approximated by a parabola indicating a continuously increasing period.

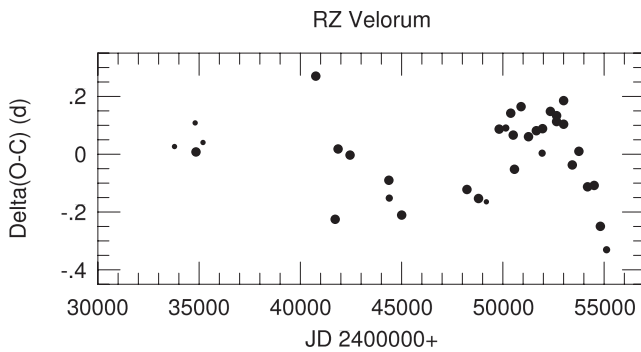


**Figure 7.**  $\Delta(O-C)$  diagram of RZ Vel.

**Table 7.** RV values of RZ Vel from the SSO spectra. (This is only a portion of the full version available online as Supporting Information.)

| JD <sub>☉</sub><br>240 0000 + | $v_{\text{rad}}$<br>(km s <sup>-1</sup> ) |
|-------------------------------|---|
| 533 07.2698                   | 4.2                                       |
| 533 10.2504                   | 1.4                                       |
| 533 12.2073                   | 9.0                                       |
| 533 64.2062                   | 49.6                                      |
| 533 67.1823                   | 27.5                                      |
| ...                           | ...                                       |

is increasing. Continuous period variations (of either sign) often occur in the pulsation of long-period Cepheids (Szabados 1983).

Fig. 7 shows the O–C residuals after subtracting the parabolic fit defined by equation (2). If the wave-like fluctuation seen in this  $\Delta(O - C)$  diagram turns out to be periodic, it would correspond to a light-time effect in a binary system. In line with the recent shortening in the pulsation period, the current value of the pulsation period is  $20.396\,671 \pm 0.000\,200$  d (after JD 245 2300).

**Binarity of RZ Vel.** There are several data sets of RV observations available in the literature for RZ Vel: those published by Stibbs (1955), Lloyd Evans (1968, 1980), Coulson & Caldwell (1985), Bersier (2002) and Nardetto et al. (2006). Our individual RV data are listed in Tables 7 and 8.

Based on these data, the RV phase curve has been constructed using the 20.398 532 d pulsation period appearing in equation (2). In view of the complicated pattern of the O–C diagram, the RV

**Table 8.** CORALIE velocities of RZ Vel. (This is only a portion of the full version available online as Supporting Information.)

| JD <sub>☉</sub><br>240 0 000 + | $v_{\text{rad}}$<br>(km s <sup>-1</sup> ) | $\sigma$<br>(km s <sup>-1</sup> ) |
|--------------------------------|---|-----------------------------------|
| 556 54.5528                    | −3.08                                     | 0.02                              |
| 556 56.6626                    | 5.23                                      | 0.01                              |
| 556 57.6721                    | 9.86                                      | 0.02                              |
| 556 59.6585                    | 18.85                                     | 0.03                              |
| 556 62.5137                    | 31.50                                     | 0.01                              |
| ...                            | ...                                       | ...                               |

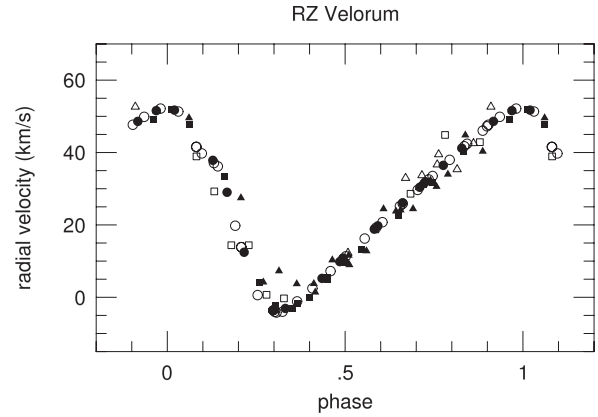


**Figure 8.** RV phase curve of RZ Vel. Data obtained between 1996 and 2013 are included in this plot. The meaning of various symbols is explained in the text.

data have been folded on by taking into account the proper phase correction for different data series. The merged RV phase curve is plotted in Fig. 8. For the sake of clarity, RV data obtained before JD 245 0000 have not been plotted here because of the wider scatter of these early RV data, but the  $\gamma$ -velocities were determined for each data set. The individual data series are denoted by different symbols: filled squares mean data by Bersier (2002), empty squares those by Nardetto et al. (2006), and our 2005, 2006, 2012 and 2013 data are denoted by filled triangles, empty triangles, filled circles and empty circles, respectively. The wide scatter in this merged RV phase curve plotted in Fig. 8 is due to a variable  $\gamma$ -velocity.

The  $\gamma$ -velocities determined from each data set (including the earlier ones) are listed in Table 9 and are plotted in Fig. 9. The plot implies that RZ Vel is really an SB as suspected by Bersier (2002) based on a much poorer observational material (before JD

**Table 9.**  $\gamma$ -velocities of RZ Vel.

| Mid-JD<br>240 0000+ | $v_{\gamma}$<br>(km s <sup>-1</sup> ) | $\sigma$<br>(km s <sup>-1</sup> ) | Data source               |
|---------------------|---------------------------------------|-----------------------------------|---------------------------|
| 340 09              | 25.5                                  | 1.5                               | Stibbs (1955)             |
| 403 28              | 22.1                                  | 1.5                               | Lloyd Evans (1968, 1980)  |
| 421 86              | 29.2                                  | 1.0                               | Coulson & Caldwell (1985) |
| 441 86              | 22.6                                  | 1.0                               | Coulson & Caldwell (1985) |
| 447 36              | 24.4                                  | 1.0                               | Coulson & Caldwell (1985) |
| 503 17              | 25.1                                  | 0.2                               | Bersier (2002)            |
| 531 84              | 24.0                                  | 0.5                               | Nardetto et al. (2006)    |
| 534 44              | 26.9                                  | 0.6                               | Present paper             |
| 537 83              | 28.8                                  | 1.0                               | Present paper             |
| 557 09              | 25.6                                  | 0.1                               | Present paper             |
| 560 38              | 25.3                                  | 0.1                               | Present paper             |



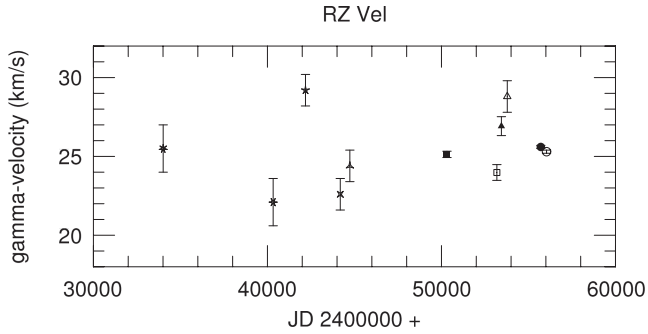


**Figure 9.**  $\gamma$ -velocities of RZ Vel. The symbols for the different data sets are the same as in Fig. 8.

245 0500). An orbital period of about 5600–5700 d is compatible with the data pattern in both Figs 7 and 9, but the phase relation between the light-time effect fit to the  $\Delta(O - C)$  curve and the orbital RV variation phase curve obtained with this formal period is not satisfactory.

### 3.3 BG VELORUM

*Accurate value of the pulsation period.* The brightness variability of BG Vel (HD 78801,  $\langle V \rangle = 7.69$  mag) was revealed by Cannon (Pickering 1909). Much later O’Leary (1937) independently discovered its light variations, but he also revealed the Cepheid nature and determined the pulsation period based on photographic plates obtained at the Riverview College Observatory. Van Houten (1950) also observed this Cepheid photographically in Johannesburg, but these early data are unavailable; therefore, we only mention their studies for historical reasons.

This Cepheid is a fundamental-mode pulsator. The O–C differences of BG Vel calculated for brightness maxima are listed in Table 10. These values have been obtained by taking into account the constant and linear terms of the following weighted parabolic fit:

$$C = 245\,3031.4706 + 6.923\,843 \times E + 2.58 \times 10^{-8} E^2 \pm 0.0020 \pm 0.000\,007 \pm 0.27 \times 10^{-8} \quad (3)$$

The parabolic nature of the O–C diagram, i.e. the continuous increase in the pulsation period, is clearly seen in Fig. 10. This parabolic trend corresponds to a continuous period increase of  $(5.16 \pm 0.54) \times 10^{-8}$  d cycle $^{-1}$ , i.e.  $\Delta P = 0.000\,272$  d century $^{-1}$ . This tiny period increase has also been caused by stellar evolution as in the case of RZ Vel.

The fluctuations around the fitted parabola in Fig. 10 do not show any definite pattern: see the  $\Delta(O - C)$  diagram in Fig. 11.

*Binarity of BG Vel.* There are earlier RV data of this Cepheid obtained by Stibbs (1955) and Lloyd Evans (1980). Variability in the  $\gamma$ -velocity is seen in the merged phase diagram of all RV data of BG Vel plotted in Fig. 12. In this diagram, our 2005–2006 data (listed in Table 11) are represented with the empty circles, while 2012–2013 data (listed in Table 12) are denoted by the filled circles, the triangles represent Stibbs’ data, and the  $\times$  symbols refer to Lloyd Evans’ data. Our RV data have been folded with the period given in the ephemeris, equation (3), omitting the quadratic term. Data obtained by Stibbs and Lloyd Evans have been phased with the same period, but a proper correction has been applied to allow for the phase shift due to the parabolic O–C graph.

**Table 10.** O–C values of BG Vel (description of the columns is given in Section 3.1).

| JD $_{\odot}$<br>2 400 000 + | $E$   | O–C     | $W$ | Data source                 |
|------------------------------|-------|---------|-----|-----------------------------|
| 348 56.5526                  | –2625 | 0.1699  | 3   | Walraven et al. (1958)      |
| 352 37.3813                  | –2570 | 0.1872  | 3   | Irwin (1961)                |
| 407 48.6592                  | –1774 | 0.0861  | 3   | Pel (1976)                  |
| 428 53.4433                  | –1470 | 0.0219  | 3   | Dean (1977)                 |
| 443 00.5426                  | –1261 | 0.0380  | 3   | Berdnikov (2008)            |
| 481 36.3167                  | –707  | 0.0031  | 3   | <i>Hipparcos</i> (ESA 1997) |
| 486 27.9239                  | –636  | 0.0174  | 3   | <i>Hipparcos</i> (ESA 1997) |
| 503 79.6329                  | –383  | –0.0058 | 3   | Berdnikov (2008)            |
| 505 73.4987                  | –355  | –0.0076 | 3   | Berdnikov (2008)            |
| 509 05.8549                  | –307  | 0.0041  | 3   | Berdnikov (2008)            |
| 512 65.9127                  | –255  | 0.0221  | 3   | Berdnikov (2008)            |
| 516 46.7345                  | –200  | 0.0325  | 3   | Berdnikov (2008)            |
| 519 37.5210                  | –158  | 0.0176  | 3   | ASAS (Pojmanski 2002)       |
| 519 58.2712                  | –155  | –0.0038 | 3   | Berdnikov (2008)            |
| 523 59.8640                  | –97   | 0.0062  | 3   | ASAS (Pojmanski 2002)       |
| 523 59.8778                  | –97   | 0.0200  | 3   | Berdnikov (2008)            |
| 526 50.6575                  | –55   | –0.0017 | 3   | Berdnikov (2008)            |
| 527 26.8212                  | –44   | –0.0003 | 3   | ASAS (Pojmanski 2002)       |
| 530 03.7916                  | –4    | 0.0164  | 3   | Berdnikov (2008)            |
| 530 31.4758                  | 0     | 0.0052  | 3   | ASAS (Pojmanski 2002)       |
| 533 36.1201                  | 44    | 0.0004  | 1   | <i>INTEGRAL</i> OMC         |
| 534 60.7390                  | 62    | –0.0099 | 3   | ASAS (Pojmanski 2002)       |
| 537 79.2202                  | 108   | –0.0254 | 3   | ASAS (Pojmanski 2002)       |
| 541 80.8337                  | 166   | 0.0052  | 3   | ASAS (Pojmanski 2002)       |
| 545 40.8499                  | 218   | –0.0185 | 3   | ASAS (Pojmanski 2002)       |
| 548 38.5810                  | 261   | –0.0126 | 3   | ASAS (Pojmanski 2002)       |
| 551 43.2425                  | 305   | –0.0002 | 2   | ASAS (Pojmanski 2002)       |

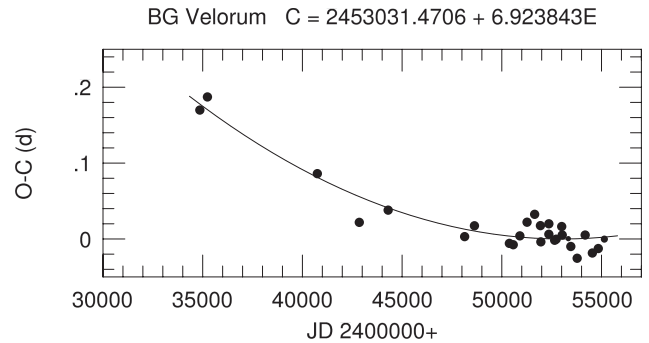


**Figure 10.** O–C diagram of BG Vel. The plot can be approximated by a parabola indicating a continuously increasing pulsation period.

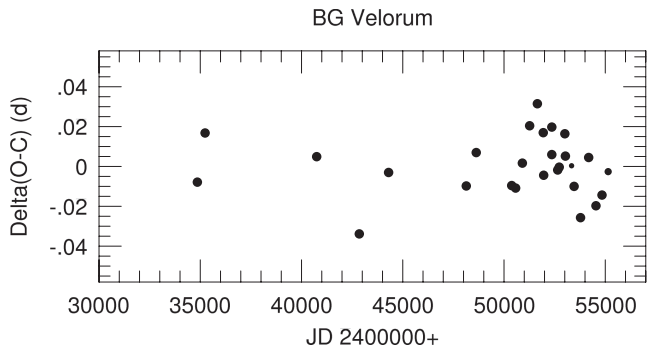


**Figure 11.**  $\Delta(O - C)$  diagram of BG Vel.

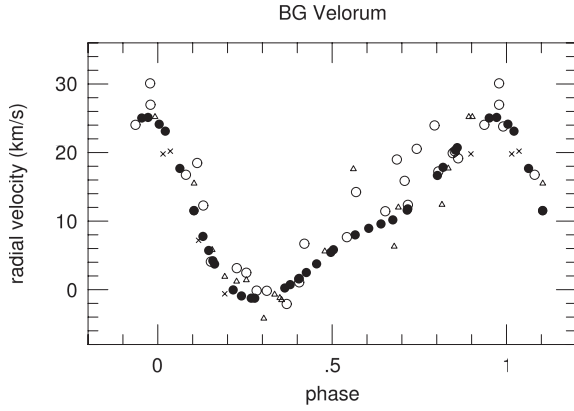


**Figure 12.** Merged RV phase curve of BG Vel. There is an obvious shift between the  $\gamma$ -velocities valid for the epoch of our data obtained in 2005–2006 and 2012–2013 (empty and filled circles, respectively). The other symbols are explained in the text.

**Table 11.** RV values of BG Vel from the SSO spectra. (This is only a portion of the full version available online as Supporting Information.)

| JD <sub>☉</sub><br>2400 000 + | $v_{\text{rad}}$<br>(km s <sup>-1</sup> ) |
|-------------------------------|---|
| 533 12.2372                   | 17.3                                      |
| 533 64.2219                   | −0.2                                      |
| 533 67.1992                   | 20.5                                      |
| 534 51.0000                   | 20.0                                      |
| 534 52.0021                   | 23.8                                      |

**Table 12.** CORALIE velocities of BG Vel. (This is only a portion of the full version available online as Supporting Information.)

| JD <sub>☉</sub><br>240 0000 + | $v_{\text{rad}}$<br>(km s <sup>-1</sup> ) | $\sigma$<br>(km s <sup>-1</sup> ) |
|-------------------------------|---|-----------------------------------|
| 559 37.7555                   | 24.13                                     | 0.02                              |
| 559 38.6241                   | 7.77                                      | 0.02                              |
| 559 39.6522                   | −1.25                                     | 0.01                              |
| 559 41.6474                   | 7.99                                      | 0.10                              |
| 559 42.6917                   | 11.78                                     | 0.03                              |

The  $\gamma$ -velocities determined from the individual data sets are listed in Table 13 and plotted in Fig. 13. Since no annual shift is seen in the  $\gamma$ -velocities between two consecutive years (2005–2006 and 2012–2013), the orbital period cannot be short; probably, it exceeds a thousand days.

Similarly to the case of LR TrA, BG Vel is also characterized by an excessive value for the ratio of RV to photometric amplitudes, indicating the possible presence of a companion (see Fig. 14).

**Table 13.**  $\gamma$ -velocities of BG Vel.

| Mid-JD<br>240 0000+ | $v_{\gamma}$<br>(km s <sup>-1</sup> ) | $\sigma$<br>(km s <sup>-1</sup> ) | Data source        |
|---------------------|---------------------------------------|-----------------------------------|--------------------|
| 340 96              | 11.4                                  | 1.5                               | Stibbs (1955)      |
| 405 45              | 8.4                                   | 1.5                               | Lloyd Evans (1980) |
| 535 72              | 12.6                                  | 0.6                               | Present paper      |
| 560 43              | 10.3                                  | 0.1                               | Present paper      |

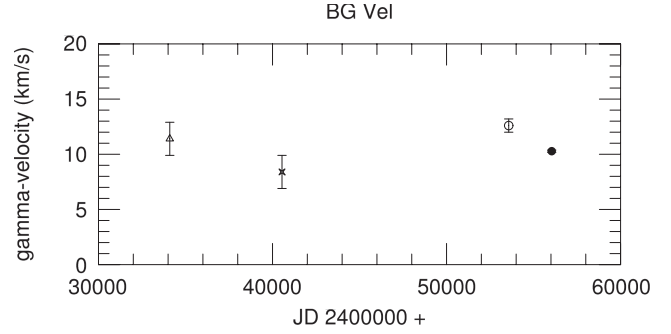


**Figure 13.**  $\gamma$ -velocities of BG Vel. The symbols for the different data sets are the same as in Fig. 12.

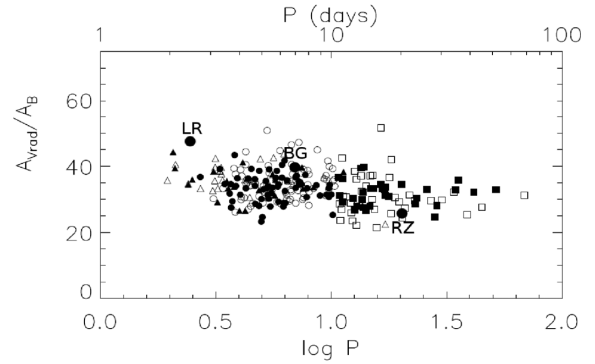


**Figure 14.** The slightly excessive value of the  $A_{V_{\text{RAD}}}/A_B$  amplitude ratio of LR TrA and BG Vel (large circles) with respect to the average value characteristic at the given pulsation period is an independent indication of the presence of a companion star. This is a modified version of fig. 4(f) of Klagyivik & Szabados (2009). The open symbols in the original figure correspond to known binaries and the filled symbols to Cepheids without known binarity. For the meaning of various symbols, see Klagyivik & Szabados (2009).

## 4 CONCLUSIONS

We pointed out that three bright southern Galactic Cepheids, LR TrA, RZ Vel and BG Vel, have a variable  $\gamma$ -velocity, implying their membership in SB systems. RV values of other target Cepheids observed with the same equipment in 2005–2006 and 2012 testify that this variability in the  $\gamma$ -velocity is not of instrumental origin, nor an artefact caused by the analysis.

The available RV data are insufficient to determine the orbital period and other elements of the orbits. However, some inferences can be made from the temporal variations of the  $\gamma$ -velocity. An orbital period of 5600–5700 d of the RZ Vel system is compatible with the data pattern. In the case of BG Vel, short orbital periodicity can be ruled out. For LR TrA, even the range of the possible orbital periods remains uncertain.

The value of the orbital period for SB systems involving a Cepheid component is often unknown: according to the online data base (Szabados 2003a) the orbital period has been determined for about 20 per cent of the known SB Cepheids. The majority of known orbital periods exceed a thousand days.

A companion star may have various effects on the observable photometric properties of the Cepheid component. Various pieces of evidence of duplicity based on the photometric criteria are discussed by Szabados (2003b) and Klagyivik & Szabados (2009). As to our targets, there is no obvious sign of a companion from optical multicolour photometry. This indicates that the companion

star cannot be much hotter than any of the Cepheids discussed here. There is, however, a phenomenological parameter, viz. the ratio of RV to photometric amplitudes (Klagyivik & Szabados 2009) whose excessive value is a further hint at the probable existence of a companion for both LR TrA and BG Vel (see Fig. 14). Moreover, the *IUE* spectra of bright Cepheids analysed by Evans (1992) gave a constraint on the temperature of a companion to remain undetected in the ultraviolet spectra: in the case of RZ Vel, the spectral type of the companion cannot be earlier than A7, while for BG Vel this limiting spectral type is A0. Further spectroscopic observations are necessary to characterize these newly detected SB systems.

Our findings confirm the previous statement by Szabados (2003a) about the high percentage of binaries among classical Cepheids and the observational selection effect hindering the discovery of new cases (see also Fig. 1).

Regular monitoring of the RVs of a large number of Cepheids will be instrumental in finding more SBs among Cepheids. RV data to be obtained with the *Gaia* astrometric space probe (expected launch: 2013 September) will certainly result in revealing new SBs among Cepheids brighter than the 13–14th magnitude (Eyer et al. 2012). In this manner, the ‘missing’ SBs among Cepheids inferred from Fig. 1 can be successfully revealed within few years.

## ACKNOWLEDGEMENTS

This project has been supported by ESTEC Contract No. 4000106398/12/NL/KML, Hungarian OTKA Grants K76816, K83790, K104607 and MB08C 81013, as well as the European Community’s Seventh Framework Program (FP7/2007–2013) under grant agreement no. 269194, and the ‘Lendület-2009’ Young Researchers Program of the Hungarian Academy of Sciences. AD was supported by a Hungarian Eötvös Fellowship. AD has also been supported by a János Bolyai Research Scholarship of the Hungarian Academy of Sciences. AD is very thankful to the staff at The Lodge in the Siding Spring Observatory for their hospitality and very nice food, making the time spent there lovely and special. Part of the research leading to these results has received funding from the European Research Council under the European Community’s Seventh Framework Program (FP7/2007–2013)/ERC grant agreement no. 227224 (PROSPERITY). The *INTEGRAL* photometric data, pre-processed by ISDC, have been retrieved from the OMC Archive at CAB (INTA-CSIC). We are indebted to Stanley Walker for sending us some unpublished photoelectric observational data. Our thanks are also due to the referee and Dr Mária Kun for their critical remarks leading to a considerable improvement in the presentation of the results.

## REFERENCES

Antonello E., Poretti E., Reduzzi L., 1990, *A&A*, 236, 138  
 Baranne A. et al., 1996, *A&AS*, 119, 373  
 Berdnikov L. N., 2008, *VizieR Online Data Catalog*: II/285  
 Bersier D., 2002, *ApJS*, 140, 465  
 Coulson I. M., Caldwell J. A. R., 1985, *SAAO Circ.*, 9, 5  
 Dean J. F., 1977, *Mon. Notes Astron. Soc. South Afr.*, 36, 3  
 Dean J. F., Cousins A. W. J., Bywater R. A., Warren P. R., 1977, *Mem. R. Astron. Soc.*, 83, 69

Derekas A. et al., 2012, *MNRAS*, 425, 1312  
 Eggen O. J., 1982, *ApJS*, 50, 199  
 Eggen O. J., 1983, *AJ*, 88, 361  
 Eggen O. J., 1985, *AJ*, 90, 1297  
 Eggen O. J., Gascoigne S. C. B., Burr E. J., 1957, *MNRAS*, 117, 406  
 ESA, 1997, *The Hipparcos and Tycho Catalogues*, ESA SP-1200  
 Evans N. R., 1992, *ApJ*, 384, 220  
 Eyer L. et al., 2012, *Ap&SS*, 341, 207  
 Hertzsprung E., 1936, *Bull. Astron. Inst. Neth.*, 8, 25  
 Irwin J. B., 1961, *ApJS*, 6, 253  
 Klagyivik P., Szabados L., 2009, *A&A*, 504, 959  
 Lloyd Evans T., 1968, *MNRAS*, 141, 109  
 Lloyd Evans T., 1980, *SAAO Circ.*, 1, 257  
 Madore B. F., 1975, *ApJS*, 29, 219  
 Munari U., Sordo R., Castelli F., Zwitter T., 2005, *A&A*, 442, 1127  
 Nardetto N., Mourard D., Kervella P., Mathias Ph., Mérand A., Bersier D., 2006, *A&A*, 453, 309  
 O’Leary W., 1937, *Riverview Coll. Obs. Publ.*, 4, 49  
 Oosterhoff P. Th., 1936, *Bull. Astron. Inst. Neth.*, 8, 29  
 Pel J. W., 1976, *A&AS*, 24, 413  
 Pepe F., Mayor M., Galland F., Naef D., Queloz D., Santos N. C., Udry S., Burnet M., 2002, *A&A*, 388, 632  
 Pickering E. C., 1909, *Harvard Coll. Obs. Circ.*, 151, 1  
 Pojmanski G., 2002, *Acta Astron.*, 52, 397  
 Queloz D. et al., 2001, *The Messenger*, 105, 1  
 Ségransan D. et al., 2010, *A&A*, 511, 45  
 Sterken C., 2005, in Sterken C., ed., *ASP Conf. Ser. Vol. 335, The Light-Time Effect in Astrophysics*. Astron. Soc. Pac., San Francisco, p. 3  
 Stibbs D. W. N., 1955, *MNRAS*, 115, 363  
 Strohmeier W., Fischer H., Ott H., 1966, *Inf. Bull. Var. Stars*, 120, 1  
 Szabados L., 1983, *Ap&SS*, 96, 185  
 Szabados L., 2003a, *Inf. Bull. Var. Stars*, 5394, 1  
 Szabados L., 2003b, *Recent Res. Dev. Astron. Astrophys.*, 1, 787  
 Szabados L. et al., 2013, *MNRAS*, 430, 2018  
 van Houten C. J., 1950, *Ann. Leiden*, 20, 223  
 Walraven Th., Muller A. B., Oosterhoff P. T., 1958, *Bull. Astron. Inst. Neth.*, 14, 81

## SUPPORTING INFORMATION

Additional Supporting Information may be found in the online version of this article:

**Table 3.** RV values of LR TrA from the SSO spectra.

**Table 4.** CORALIE velocities of LR TrA.

**Table 7.** RV values of RZ Vel from the SSO spectra.

**Table 8.** CORALIE velocities of RZ Vel.

**Table 11.** RV values of BG Vel from the SSO spectra.

**Table 12.** CORALIE velocities of BG Vel. (<http://mnras.oxfordjournals.org/lookup/suppl/doi:10.1093/mnras/stt1079/-/DC1>).

Please note: Oxford University Press is not responsible for the content or functionality of any supporting materials supplied by the authors. Any queries (other than missing material) should be directed to the corresponding author for the paper.

This paper has been typeset from a  $\text{\LaTeX}$  file prepared by the author.